Chapter

Computational Study on Optoelectronic Properties of Donor-Acceptor Type Small π-Conjugated Molecules for Organic Light-Emitting Diodes (OLEDs) and Nonlinear Optical (NLO) Applications

Rania Zaier and Sahbi Ayachi

Abstract

Recently, donor-acceptor type molecule that contains electron-rich (D) and electron-deficient (A) moiety has emerged as an interesting approach of molecular design strategy to develop organic light-emitting diodes (OLEDs) and non-linear optical (NLO) devices. In this work, we report a theoretical investigation based on two donor-acceptor (D-A) type small π-conjugated molecules based on dithieno [3,2-b: 2′,3′-d] pyrrole (DTP) and anthracene derivatives. All of the theoretical calculations were performed by Density Functional Theory (DFT) approach at B3LYP/6-31 g(d) level of theory. The structural, electronic, optical and charge transfer properties were investigated. The effect of acceptor blocks (DPA and DTA) on the molecular characteristics was elucidated. The obtained results clearly show that the studied compounds exhibit non-coplanar structures with low electronic band gap values. These relevant structures exhibited important optical absorption and intense emission in the green-yellow region. NLO investigation based on static polarizability (α_0), first-order hyperpolarizability (β_0) and second-order hyperpolazabilty (γ_0) demonstrated that the studied materials exhibit excellent NLO properties. Thus, the designed materials showed promising capabilities to be utilized in OLED and NLO applications.

Keywords: DTP, Anthracene, DFT, Optical properties, OLEDs, NLO properties

1. Introduction

Recently, several categories of conjugated materials have gained significant interest due to their relevant optoelectronic characteristics for the development of a wide range of organic electronic devices [1–3]. Remarkably, organic luminescent

materials are increasingly attractive in the manufacture of organic light-emitting diodes (OLEDs) and non-linear optical (NLO) devices [4–6].

OLEDs are desirable electronic devices due to their valuable advantages of full color emission, high brightness, flexibility and operation stability [7–11]. OLEDs were greatly developed in electronic fields and showed their successful applications in digital displays, mobile phones and flat panels in TV screens [12]. Various functional units, such as fluorene [13], carbazole [14] and anthracene [15] were utilized to develop efficient luminescent materials for their prominent photoluminescence properties and simple modifications. Among these functional units, anthracene and its derivatives were widely studied as potential building blocks in the development of active materials for OLED devices [16].

Apart from OLEDs, recent studies have demonstrated the potential application of conjugated materials in NLO devices [17, 18]. NLO materials have reached large interest of the scientific community for prosperous use in technological areas such as telecommunications, optical information processing and data storage [19–21]. NLO studies have shown the design of promising organic materials for nonlinear effect based on the introduction of highly delocalized electron fragments and additional electron donor and acceptor groups for enhancing the molecular conjugation [22].

Previous works have shown that D-A (Donor-Acceptor) systems dispose a successful architecture for non-linear optics and OLEDs. Where, D-A systems exhibit large charge transfer (CT) in which the electrons located in the electron rich donor unit undergo an intra-molecular charge transfer (ICT) to the electron deficient acceptor unit [23, 24]. The present CT phenomenon leads to excellent optoelectronic characteristics that encourage the use of D-A systems in NLO and OLED applications.

Dithieno [3,2-b: 2′,3′-d] pyrrole (DTP) material has been recognized as one of the most efficient building blocks with high electron donation capacity [25, 26]. DTP building blocks have been widely incorporated into a variety of materials for the aim of reducing the band gap, improving the mobility of charge carriers, and reinforcing solution and solid state fluorescence.
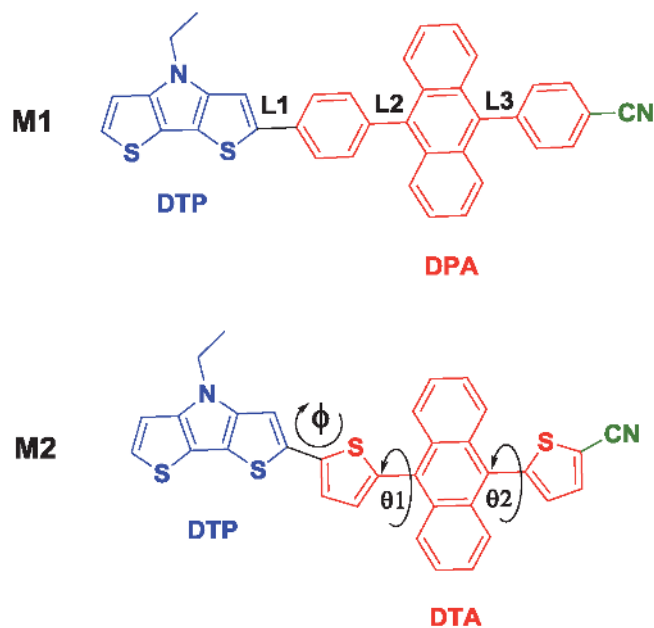
Figure 1.
Molecular structures of the investigated compounds.

Equally, anthracene has attracted significant attention to the construction of organic luminescent materials due to its unique features. Where, anthracene derivatives such as 9,10-diphenylanthracene (DPA) and 9,10-di(thiophen-2-yl)anthracene (DTA) have exhibited remarkable electronic and light-emitting properties to be applied in optical applications [27, 28].

In the present work, we have developed a theoretical investigation based on new D-A type small molecules for NLO and OLED applications. As mentioned in **Figure 1**, we have used DTP as an electron donor block and derivatives from DPA and DTA as an electron acceptor block. The addition of a strong electron withdrawing group as cyano group is for the reason of enhancing the polarization and improving the π-electrons delocalization [29].

A theoretical computational study using density functional theory (DFT) approach introduce excellent tools to predict the optoelectronic properties of molecular systems as well as the design of new materials for OLED and NLO devices [30]. Hence, the designed materials will be theoretically investigated and discussed to envisage the reliability for OLED and NLO applications.

2. Computational methods

Theoretical calculations were performed using Density Functional Theory (DFT) approach implemented in Gaussian 09 software [31]. Previous studies have shown that DFT//B3LYP/6-31 g(d) method gives better accuracy in investigating the photo-physical properties of materials based on DTP and anthracene [32, 33]. Structural properties such as dihedral angles, torsion angles and bridge bond lengths were firstly investigated based on the geometry optimization of **M1** and **M2** in their ground states. Vibrational calculations were carried out to confirm the stable conformers with no imaginary frequencies. Frontier molecular orbitals (FMOs) and electron density difference (EDD) contour plots were carried out to examine the electron delocalization within the conjugated frameworks. The absorption and emission spectra were simulated using Time Dependent DFT (TD-DFT) at B3LYP/6-31 g(d) level. Photoluminescence color coordinates of **M1** and **M2** were determined using International Commission on Illumination (usually abbreviated CIE for its French name, Commission internationale de l'éclairage) process. Bilayer OLED devices are designed based on the optoelectronic properties of the studied molecules. Hole and electron charge transfer properties (λ_h, λ_e) were carried out on neutral, anionic and cationic states. The NLO properties involving the electric dipole moment (μ), the polarizability (α), the first order hyperpolarizability (β) and the second order hyperpolarizability (γ) were investigated.

3. Results and discussion

3.1 Ground state optimized geometries

The development of high performance luminescent materials is principally based on the enhancement of π-electrons delocalization within the conjugated architectures. In fact, the geometric structure gives an idea about the delocalization of the π-electrons as well as the charge transfer (CT) within the conjugated structure [34].

Hence, the ground state geometries of the studied materials were optimized using DFT//B3LYP/6-31 g(d) method in gaseous phase. The optimized geometries of **M1** and **M2** are illustrated in **Figure 2** and the geometric parameters involving bond lengths, torsion angles and dihedral angles are listed in **Table 1**.
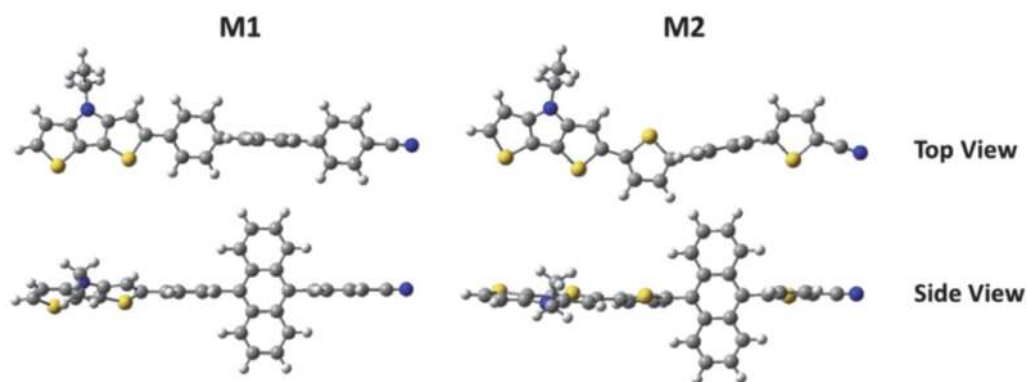
Figure 2.
Ground state optimized geometries at B3LYP/6-31 g(d) level for the studied molecules.

	M1	M2
Bond length (Å)		
L1	1.46	1.44
L2	1.49	1.48
L3	1.49	1.48
Torsion angle (deg.)		
Θ1	119.96	119.88
Θ2	119.83	119.68
Torsion angle (deg.)		
Φ	25.67	17.24

Table 1.
Optimized ground state geometry parameters of the studied molecules.

The considered materials exhibit non-coplanar structures (**Figure 2**). There are large torsion angles around 119° between anthracene and phenyl ring in **M1** and between anthracene and thiophene ring in **M2** (**Table 1**) which is a characteristic property of compounds based substituted anthracene [23, 35].

Furthermore, as mentioned in **Figure 1**, the characteristic bridge bonds between the donor and acceptor blocks (L1) and between the different groups of the acceptor units (L2 and L3) were calculated to have an idea about the charge transfer (CT) in the conjugated backbone. The calculated lengths of bond L1 were found equal to 1.46 and 1.44 Å for **M1** and **M2**, respectively. While, the bond lengths of L2 and L3 were found about 1.49 Å for **M1** and about 1.48 Å for **M2**. The calculated values are located in the interval between C-C single bond length (C-C = 1.54 Å) and C=C double-bond length (C=C = 1.33 Å) showing the high π-electron delocalization and interesting intra-molecular charge transfer (ICT) within the framework [36].

The structural analysis suggests that the studied compounds exhibit good conjugated structures with high π-electron delocalization, which is important for applications in organic electronic devices.

3.2 Frontier molecular orbitals (FMOs)

The electronic properties of the studied molecules are examined based on the frontier molecular orbital (FMOs) analysis. The highest occupied molecular orbitals

(HOMOs) and the lowest unoccupied molecular orbitals (LUMOs) contour plots were carried out using the DFT//B3LYP/6-31 g(d) method at the optimized ground state geometries. The energy values of HOMOs, LUMOs and band gap energies are listed in **Table 2**. The HOMOs and LUMOs distributions are illustrated in **Figure 3**.

As depicted in **Figure 3**, the HOMOs are mostly located over the DTP unit while the LUMOs are distributed over the DPA and DTA acceptor units that indicate the important electron charge transfer from the donor to acceptor moieties. Hence, the FMOs analysis has shown the considerable charge transfer taking place within the designed molecules.

The band gap energies are calculated from the difference between the HOMO and LUMO energy levels at DFT//B3LYP/6-31 g(d) method. The band gap energies are about 3.16 eV and 2.81 eV for **M1** and **M2**, respectively. These lower values of band gaps with the FMOs distributions demonstrate the presence of a significant intra-molecular charge transfer (ICT) that leads to enhance the electronic properties [37].

Density of states (DOS) is a helpful tool to examine the delocalization of π-electrons in the compound. The DOS plots were determined by DFT//B3LYP/6-31 g (d) method at the ground state geometry and illustrated in **Figure 4**. DOS plots of **M1** and **M2** show a large overlapping of electronic energy levels that indicates the high electron delocalization. In fact, the high electron delocalization within these materials could be explained by the mutual reactions of donor and acceptor constructive blocks.

To better understand the delocalization of π-electrons, electron density difference (EDD) was simulated between the ground state (S_0) and the first excited state (S_1). As seen in **Figure 5**, the EDD plots contain blue regions referring to electron density depletion and purple regions referring to electron density increment.

Hence, the regions of electron increment density are mainly located over the DPA and DTA blocks. While, the DTP block presents the region of depleted free carriers (depletion region). These observations decline the effective electron transfer from donor to acceptor units within the studied materials.
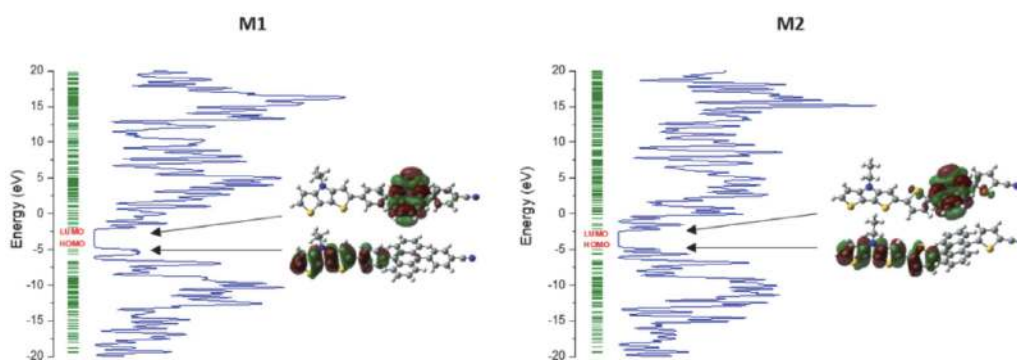
Compound	E_{HOMO-1} (eV)	E_{HOMO} (eV)	E_{LUMO} (eV)	E_{LUMO+1} (eV)	ΔE_{gap} (eV)
M1	−5.36	−5.04	−1.88	−1.41	3.16
M2	−5.57	−4.97	−2.16	−1.64	2.81

Table 2.
*DFT//B3LYP/6-31 g(d) calculated electronic properties of **M1** and **M2** molecules.*
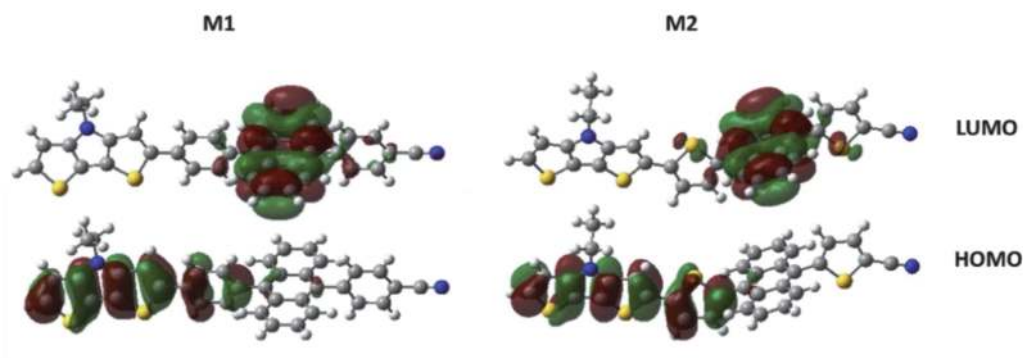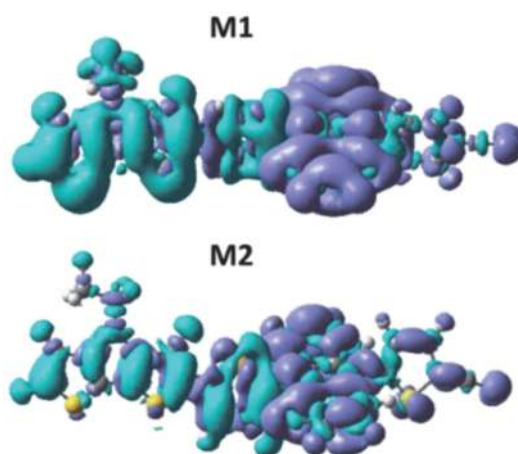

Figure 3.
Frontier molecular orbitals in the optimized ground state for the studied molecules.

Figure 4.
Density of states (DOS) plots of the studied materials.

Figure 5.
*Electron density difference (EDD) contour plots of the studied materials.*

3.3 Optical properties

3.3.1 Optical absorption properties

The optical absorption properties of **M1** and **M2** have been investigated based on the simulated UV–Vis optical absorption spectra using TD-DFT method at 6-31 g(d) basis set. The obtained optical absorption curves with their Gaussian fitting peaks are given in **Figure 6**. The simulated corresponding maximum absorption wavelengths (λ_{max}^{abs}), the electronic transition energy (Eex), the oscillator strength (f), the full-width at half maximum (FWHM) and the main electronic transitions are listed in **Table 3**.

As it can be seen from **Figure 6**, the studied molecules exhibit large and intense absorption bands in the visible zone ranging from 300 nm to 500 nm. These electronic transitions are defined as $\pi \rightarrow \pi^*$ transitions associated with the electron migration from the HOMOs mainly located over the DTP units to the LUMOs mainly concentrated over the anthracene units [38].

From **Table 3**, the maximum absorption wavelengths (λ_{max}^{abs}) of **M1** and **M2** are found at 442 nm and 406 nm, respectively. The full-width at half maximum FWHM referring to the main absorption band for **M1** is found higher than that of **M2** (FWHM (**M1**) = 76.96 > FWHM (**M2**) = 58.70). This result shows the role played by the acceptor block in improving the optical absorption properties.
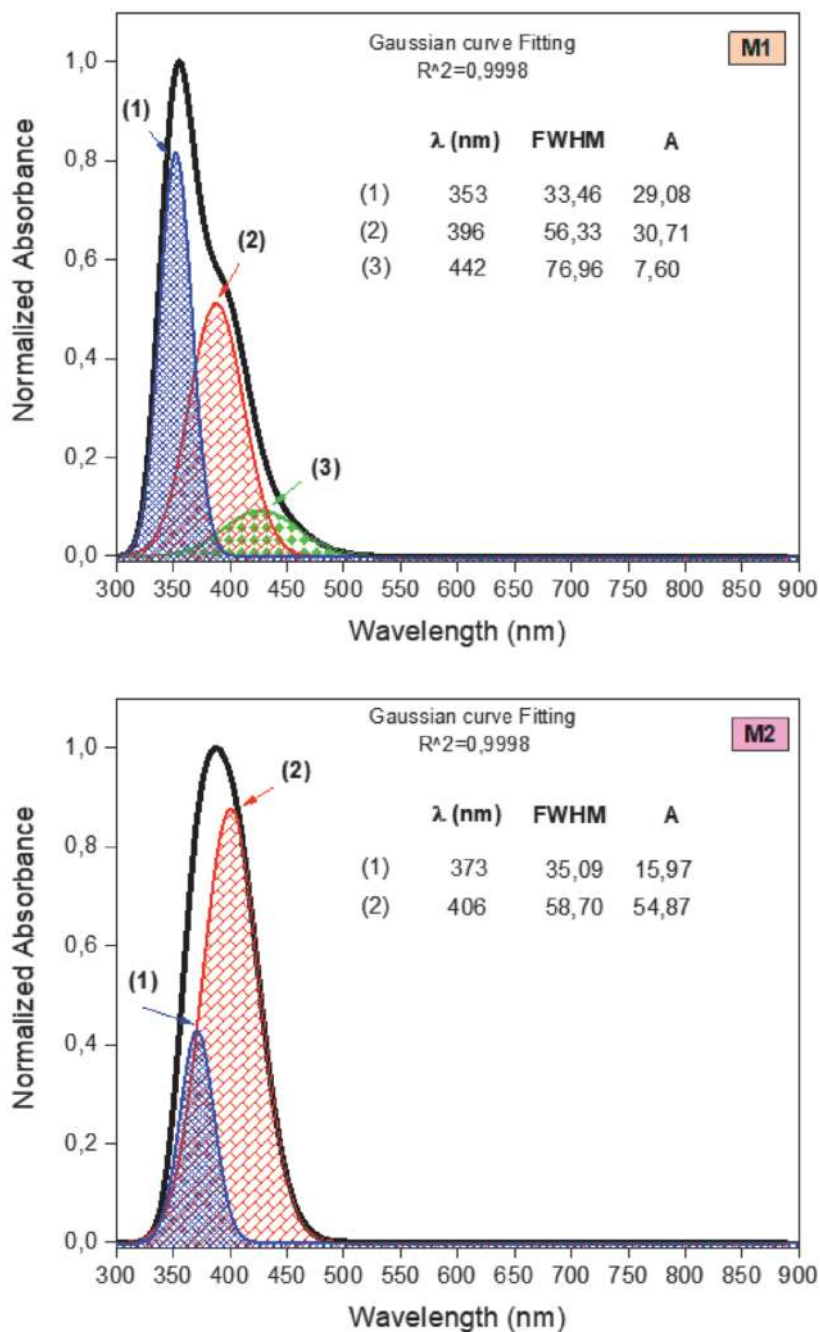
Figure 6.
*Optical absorption spectra of **M1** and **M2** with fitting Gaussian peaks obtained at DFT//B3LYP/6-31 g(d) level.*

From the optical absorption analysis, it is obvious that the acceptor block configuration contributes significantly in enhancing the absorption properties of conjugated materials.

3.3.2 Emission properties

The emission properties of **M1** and **M2** are simulated on their optimized geometries at the first excited state by means of TD-DFT//B3LYP/6-31 g(d) method. The

Compound	λ_{max}^{abs} (nm/eV)	f (a.u)	FWHM (nm)	Main electronic transitions
M1	442/2.80	0.05	76.96	H→L (99%)
	396/3.12	0.38	56.33	H-1→L (93%), H→L + 1 (4%)
	353/3.51	0.71	33.46	H→L + 2 (81%), H-2→L (9%)
M2	406/3.08	0.63	58.70	H-1→L (85%), H→L + 2 (12%)
	373/3.32	0.67	35.09	H→L + 2 (85%), H-1→L (12%)

Table 3.
Maximum absorption wavelengths λ_{max}^{abs} (nm), electronic transition energy, Eex (eV), oscillator strength f (a.u), full-width at half maximum FWHM (nm) and main electronic transitions calculated at B3LYP/6-31 g(d) level.

emission spectra with their fitting Gaussian peaks are depicted in **Figure 7** and the corresponding emission characteristics are listed in **Table 4**.

As it can be seen from **Figure 7**, the studied materials exhibit large emission bands with maximum emission wavelengths of 478 nm and 554 nm for **M1** and **M2**, respectively. As mentioned in **Table 4**, the emission spectrum of **M2** exhibits larger FWHM comparing to **M2** which indicates the effect of acceptor moiety in enhancing the emission properties.

The photoluminescence chromaticity coordinates of **M1** and **M2** were carried out according to the CIE 1931 diagram. As illustrated in **Figure 8**, the CIE coordinates are found upon (x: 0.45, y: 0.45) and (x: 0.32, y: 0.43) for **M1** and **M2**, respectively. Hence, **M1** displays a pure green color while **M2** displays a pure yellow color.

From the emission investigation, it is revealed that the studied materials are promising materials for OLED applications. Indeed, OLEDs as they are promising organic electronic devices present the subject of intense research. The efficient OLED operation requires balanced charge injection, charge transport and charge recombination within the electronic device [39].

The considered materials exhibit appropriate optoelectronic characteristics allowing their use as emitting layers in two layers OLED device. Alq$_3$ (Tris (8-hydroxyquinoline) aluminum) is a suitable material to act as an electron transport layer [40] with respect to the LUMO energy levels of **M1** and **M2** (See **Figure 8**).

Radiative lifetime (τ) introduces the average time of the stay of a molecule at the excited state before a photon-emission. The lower value of τ leads to a relevant emission of the conjugated material. The radiative lifetime τ could be determined according to the following expression [41]:

$$\tau = \frac{C^3}{2(E_{flu})^2 f}$$

(1)

Where, c, E_{flu} and f represent the velocity of light, the fluorescent energy and the oscillator strength, respectively.

The radiative lifetime values are of 10.12 ns and 5.46 ns for **M1** and **M2**, respectively. The small values of τ denote the efficient light emission of these materials. The findings of the present report corroborate a slight difference in radiative lifetime values which are explained by the effect of DPA and DTA acceptor blocks within the conjugated structures.

According to these results and compared to some previous studies reported in Refs. [28, 42], it is revealed that **M1** and **M2** exhibit promising optoelectronic properties for high performance OLED devices.
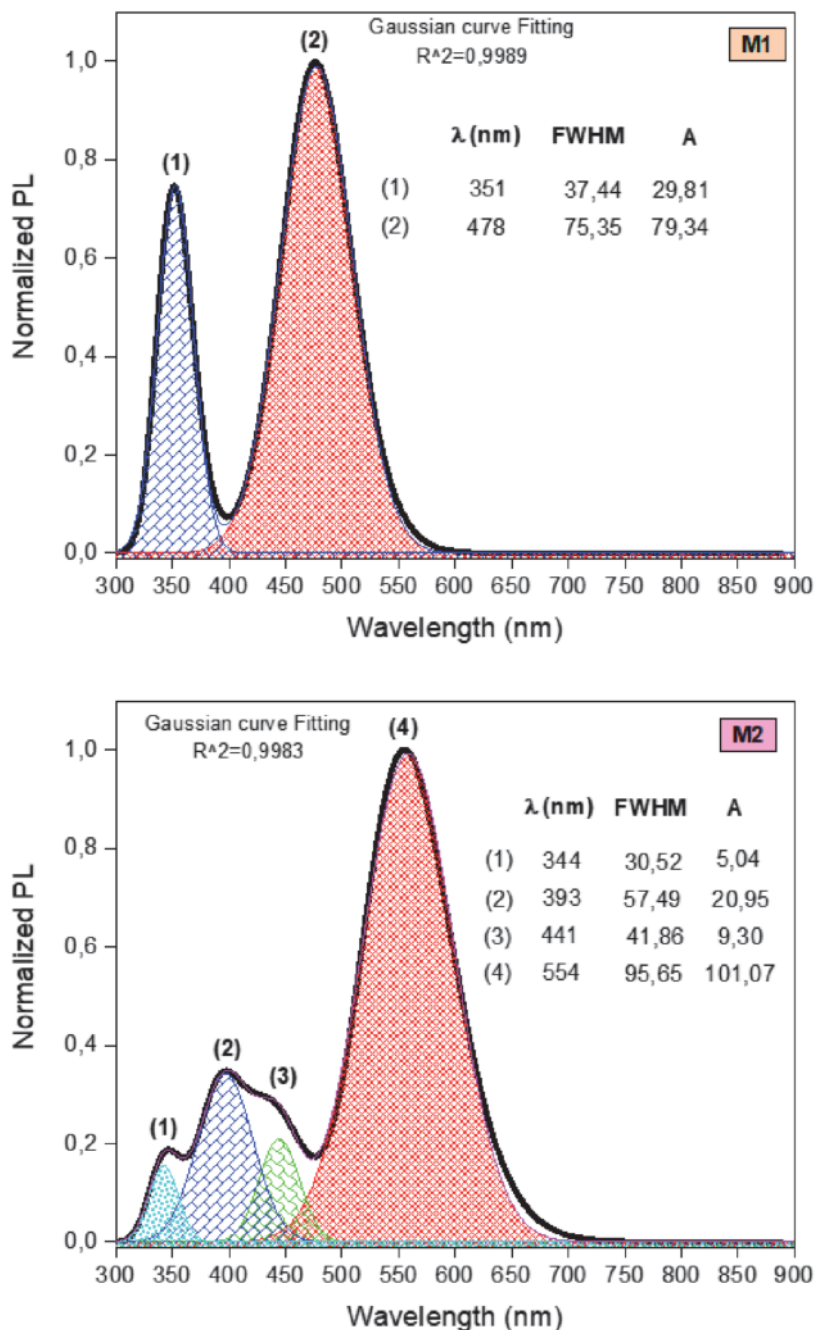
Figure 7.
*Emission spectra of **M1** and **M2** with fitting Gaussian peaks obtained at DFT//B3LYP/6-31 g(d) level.*

3.4 Charge transfer properties

Many factors are responsible for high performance organic optoelectronic devices such as hole/electron charge transfer balance. The reorganization energies of holes and electrons (λ_h and λ_e) together with the ionization potential (IP) and the electron affinity (EA) have been calculated to evaluate the hole/electron transfer abilities. The reorganization energies were carried out from neutral, cationic and anionic geometries, as detailed in **Figure 9**.

The reorganization energies of holes and electrons can be calculated following the expression above [43]:

Compound	λ_{max}^{em} (nm/eV)	f (a.u)	FWHM (nm)	Main transition	τ (ns)
M1	478/2.59	0.34	75.35	L→H (98%)	10.12
	351/3.53	0.27	37.44	L→H-2 (90%)	
M2	554/2.23	0.85	95.65	L→H (99%)	5.46
	441/2.81	0.21	41.86	L→H-1(63%)	
	393/3.15	0.18	57.49	L + 1→H (40%)	
	344/3.60	0.15	30.52	L + 1→H-1 (94%)	

Table 4.
Calculated maximum emission wavelengths λ_{max}^{em} *(nm), fluorescent energy* $E_{flu}(eV)$, *oscillator strength f (a.u), full-width at half maximum FWHM (nm), main electronic transitions, stokes shift (nm) and radiative lifetime (τ).*
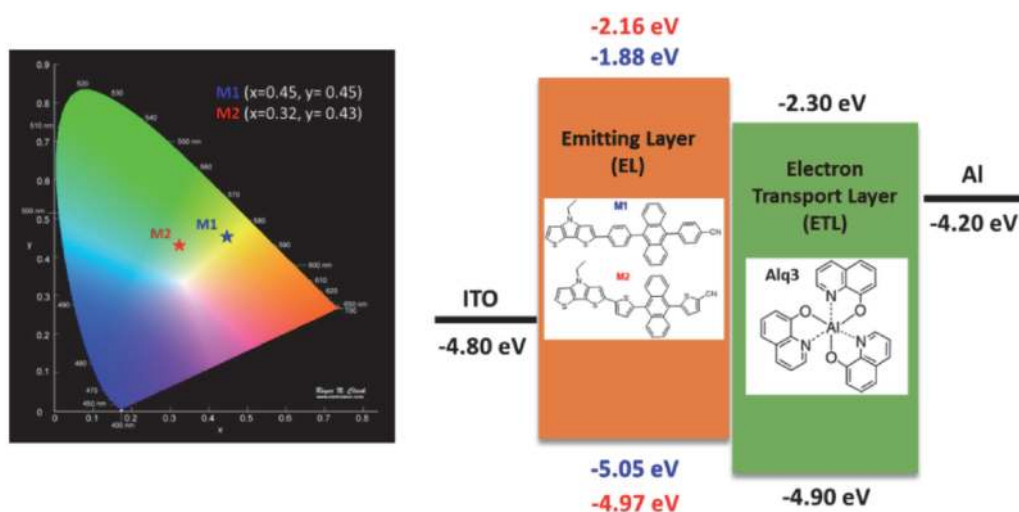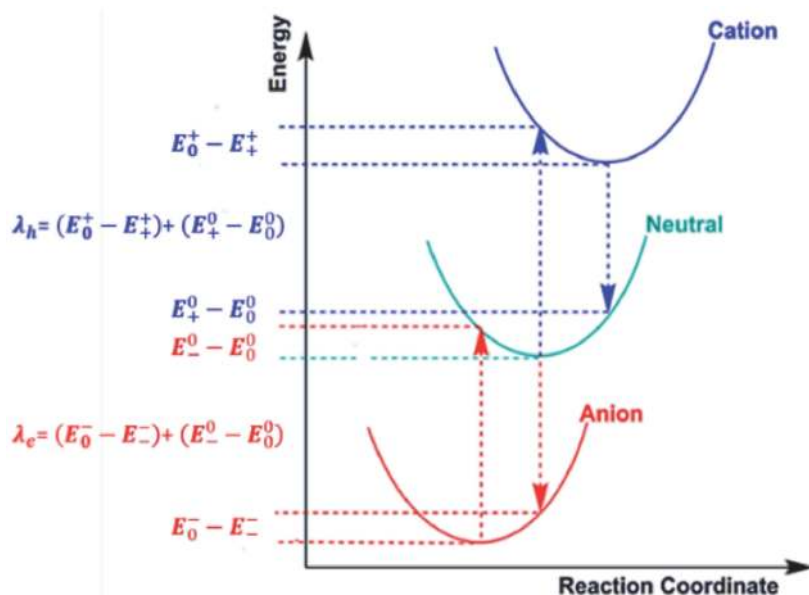

Figure 8.
CIE color coordinates for the studied materials (right), schematic structure of proposed bilayer OLED based studied materials (left).

$$\lambda_h/\lambda_e = \left(E_0^{\pm} - E_{\pm}^{\pm}\right) + \left(E_{\pm}^0 - E_0^0\right) \qquad (2)$$

Hence, $E_0^{\pm}$, $E_{\pm}^0$, $E_{\pm}^{\pm}$ and E_0^0 represent the cation/anion energy of cation/anion at neutral geometry, the energy of neutral structure in the cation/anion state, the energy of cation/anion in the cation/anion state and the energy of the neutral structure, respectively. Charge transfer parameters have been determined using DFT//B3LYP/6-31 g(d) method and the results are presented in **Table 5**. Based on the obtained results, it is found that **M1** exhibits higher hole and electron transfer abilities regarding the lower reorganization energies of hole and electron.

To get insights into the charge transport properties, the ionization potential (IP) and the electron affinity (AE) were carried out for better evaluating the electron extraction and attraction abilities, respectively [44]. In comparison with **M2**, **M1** exhibits relatively lower EA (0.94 eV versus 1.17 eV) which demonstrates that our materials exhibit low performance of grasping electrons. However, the low values of IP (6.02 eV for **M1** and 6.00 eV for **M2**) indicated the high ability of these materials to grasp hole (See **Table 5**). It is possible to better improve the mobility of charge carriers through the modification of the conjugate structure [45].

Figure 9.
Calculation details of reorganization energies from neutral cation and anion states.

Compound	IP	EA	$(E_0^+ - E_+^+)$	$(E_+^0 - E_0^0)$	$(E_0^- - E_-^-)$	$(E_-^0 - E_0^0)$	λ_h	λ_e
M1	6.02	0.94	0.171	0.129	0.283	0.144	0.300	0.427
M2	6.00	1.17	0.248	0.158	0.298	0.224	0.406	0.522

Table 5.
*Calculated charge transfer parameters (expressed in eV) of **M1** and **M2** at DFT//B3LYP/6-31 g(d) level of theory.*

Overall, the charge properties analysis of **M1** and **M2** shows that they are considered as promising materials for organic optoelectronic applications.

3.5 Nonlinear optical (NLO) properties

The principle of nonlinear optics represents the interaction between an incident electromagnetic field with a particular material leading to the generation of an electromagnetic field modified in wave number, phase or frequency [17]. NLO materials are increasingly applied in emerging technological fields such as telecommunications, optical memory, optical information processing, etc. [46].

NLO properties produced from the high delocalization of electrons within the molecule increase while increasing the molecular conjugation [47]. Further, the presence of electron donor blocks (D) and electron acceptor blocks (A) contributes to the improvement of the NLO properties [48–50]. Studies have shown that nonlinear organic optical materials possess higher optical nonlinearity compared to inorganic materials [51].

The electric dipole moment μ, the polarizabilities α, the first (β) and the second-order hyperpolarizability (γ) describe the nonlinear optical response of an isolated molecule within an electric field [52]. The total dipole moment μ_{tot}, the static polarizability α_0, the static first hyperpolarizability β_0 and the static second order hyperpolarizability γ_0 are calculated using the expressions above [22, 53]:

	M1	M2		M1	M2		M1	M2		M1	M2
μ_x	0	0	α_{xx}	63.382	74.513	β_{xxx}	5.006	5.457	γ_{xxxx}	69.828	95.548
μ_y	0	0	α_{xy}	5.051	−6.979	β_{xxy}	1.042	−1.122	γ_{yyyy}	42.211	40.665
μ_z	7.383	7.362	α_{yy}	55.263	55.263	β_{xyy}	0.220	0.139	γ_{zzzz}	831.140	624.809
μ_{tot}	7.383	7.362	α_{xz}	−33.103	−36.709	β_{yyy}	0.056	−0.034	γ_{xxyy}	3.191	1.728
			α_{yz}	−5.787	5.383	β_{xxz}	−8.816	−7.756	γ_{xxzz}	247.105	241.440
			α_{zz}	109.672	97.457	β_{xyz}	−1.979	1.656	γ_{yyzz}	11.081	10.138
			α_0	76.106	75.744	β_{yyz}	−0.475	−0.347	γ_0	293.186	253.527
						β_{xzz}	18.993	14.347			
						β_{yzz}	4.340	−3.168			
						β_{zzz}	−36.233	−24.125			
						β_0	51.851	38.145			

Table 6.
Calculated electric dipole moment μ_{tot} (D), polarizability α_o ($\times 10^{-24}$ esu), first-order hyperpolarizability β_o ($\times 10^{-30}$ esu) and second-order hyperpolarizability γ_o ($\times 10^{-36}$ esu) of the studied materials at DFT//B3LYP/ 6-31 g(d) level.

$$\mu_{tot} = \left(\mu_x{}^2 + \mu_y{}^2 + \mu_z{}^2 \right)^{\frac{1}{2}} \tag{3}$$

$$\alpha_0 = \frac{1}{3} \left(\alpha_{xx} + \alpha_{yy} + \alpha_{zz} \right) \tag{4}$$

$$\beta_0 = \left[\left(\beta_{xxx} + \beta_{xyy} + \beta_{xzz} \right)^2 + \left(\beta_{yyy} + \beta_{yzz} + \beta_{yxx} \right)^2 + \left(\beta_{zzz} + \beta_{zxx} + \beta_{zyy} \right)^2 \right]^{\frac{1}{2}} \tag{5}$$

$$\gamma_0 = (1/5) \left[\gamma_{xxxx} + \gamma_{yyyy} + \gamma_{zzzz} + 2\,\gamma_{xxyy} + 2\,\gamma_{yyzz} + 2\,\gamma_{zzxx} \right] \tag{6}$$

DFT approach is used as a reliable method for the determination of NLO properties of organic materials [54]. To get insights into the NLO properties, theoretical calculations were performed on the ground state optimized geometries of **M1** and **M2** at DFT//B3LYP/6-31 g(d) level of theory and the results are listed in **Table 6**.

From **Table 6**, the first- and second-order hyperpolarizabilities of **M2** are found lower than those of **M1** explained by the distinct electron delocalization in the conjugated structures. Thus, as compared to **M2**, it is important to note that **M1** presents the best NLO properties.

Urea is a prototypical organic molecule used as a threshold comparison value in the study of the NLO properties of molecular materials [55]. The NLO parameters of urea calculated at DFT//B3LYP/6-31 g(d) level of theory are found of: μ_{tot} = 4.259 D, α_0 =3.749 × 10–24 esu and β_0 =0.557× 10–30 esu and γ_0 = 0.746× 10–36 esu.

Compared to urea, the high values of NLO parameters of **M1** and **M2** confirm the design of high performance nonlinear optical materials.

4. Conclusion

In this study, we reported a DFT study based on structural, optoelectronic and nonlinear optical (NLO) properties of D-A small π-conjugated molecules based on

DTP and anthracene. The optimized structures have shown the non-planarity of the investigated molecules **M1** and **M2** arising from the anthracene derivatives (DPA and DTA) conjugated configuration. FMOs analysis shows the appropriate HOMO/ LUMO energy levels with the low band gap energies. To support the FMOs analysis, EDD contour plots have been computed to identify the donor and acceptor moiety within **M1** and **M2** structures. The TD-DFT study demonstrated the role played by the acceptor block in improving the absorption properties of the studied materials. The emission properties revealed an intense emission in the pure green and pure yellow for **M1** and **M2**, respectively. These molecules have shown their promising abilities to be used in OLED devices. The charge transfer properties analysis attested the relevant hole/electron transport abilities of these materials. Computed static polarizability (α_0), first-order hyperpolarizability (β_0) and second-order hyperpolazabilty (γ_0) indicated the excellent NLO properties of **M1** and **M2**. This NLO response suggested these compounds to be used as potential candidates for NLO applications. Overall, this study provided an insight into a promising D-A conjugated architecture with the role of the acceptor block on enhancing the optoelectronic performances of organic materials.

Acknowledgements

Conflict of interest

The authors declare no conflict of interest.

Author details

Rania Zaier and Sahbi Ayachi*
Laboratory of Physico-Chemistry of Materials (LR01ES19), Faculty of Sciences of Monastir (FSM), University of Monastir, Tunisia

*Address all correspondence to: ayachi_sahbi@yahoo.fr

IntechOpen

References

[1] A. Kivrak, H. Çalış, Y. Topal, H. Kivrak, M. Kuş, Synthesis of thiophenyl-substituted unsymmetrical anthracene derivatives and investigation of their electrochemical and electrooptical properties, Solar Energy Materials Solar Cells. 161 (2017) p. 31. https://doi.org/10.1016/j.solmat.2016.11.006

[2] S.R. Forrest, M.E. Thompson, Introduction: Organic Electronics and Optoelectronics, Chem. Rev. 107 (2007) p. 923. DOI: 10.1021/cr0501590

[3] R. Zaier, S. Ayachi, DFT molecular modeling studies of D-π-A-π-D type cyclopentadithiophene-diketopyrrolopyrrole based small molecules donor materials for organic photovoltaic cells, Optik. 239 (2021) p. 166787.https://doi.org/10.1016/j.ijleo.2021.166787

[4] U.R. Felscia, B.J. Rajkumar, M.B. Mary, Theoretical investigations on nonlinear fused 4-ring systems: Application to OLED and NLO devices, Synt. Met. 246 (2018) p. 31.https://doi.org/10.1016/j.synthmet.2018.09.008.

[5] S. Vijayalakshmi, S. Kalyanaraman, DFT and TD-DFT approach for the analysis of NLO and OLED applications of 9-anthraldehyde, Optik. 125 (2014) p. 2429. DOI: 10.1016/j.ijleo.2013.10.104

[6] J. George, D. Sajan, J. Alex, A. Aravind, G. Vinitha, R.J.O. Chitra, L. An experimental and computational approach to electronic and optical properties of Diglycine barium chloride monohydrate crystal: Applications to NLO and OLED, Technology, Opt. Laser Technol. 105 (2018) p. 207.https://doi.org/10.1016/j.optlastec.2018.02.056

[7] S. Yuvaraja, A. Nawaz, Q. Liu, D. Dubal, S.G. Surya, K.N. Salama, P. Sonar,Organic field-effect transistor-based flexible sensors, Chem. Soc. Rev., 49 (2020) p. 3423. https://doi.org/10.1039/C9CS00811J.

[8] L. Dou, Y. Liu, Z. Hong, G. Li, Y. Yang, Low-Bandgap Near-IR Conjugated Polymers/Molecules for Organic Electronics, Chem. Rev. 115 (2015) p. 12633. https://doi.org/10.1021/acs.chemrev.5b00165.

[9] J. Song, H. Lee, E.G. Jeong, K.C. Choi, S. Yoo, Organic Light-Emitting Diodes: Pushing Toward the Limits and Beyond, Adv. Mat. 32 (2020) p. 1907539. https://doi.org/10.1002/adma.201907539

[10] O. Ostroverkhova, Organic Optoelectronic Materials: Mechanisms and Applications, Chemical reviews. 116 (2016) p. 13279. https://doi.org/10.1021/acs.chemrev.6b00127

[11] X. Guo, M. Baumgarten, K. Müllen, Designing π-conjugated polymers for organic electronics, Prog. Poly. Sci. 38 (2013) p. 1832. https://doi.org/10.1016/j.progpolymsci.2013.09.005.

[12] B. Yang, S.K. Kim, H. Xu, Y.I. Park, H. Zhang, C. Gu, F. Shen, C. Wang, D. Liu, X. Liu, The Origin of the Improved Efficiency and Stability of Triphenylamine-Substituted Anthracene Derivatives for OLEDs: A Theoretical Investigation, ChemPhysChem. 9 (2008) p. 2601. https://doi.org/10.1002/cphc.200800513.

[13] S. Tao, Z. Peng, X. Zhang, P. Wang, C.S. Lee, S.T. Lee, Highly Efficient Non-Doped Blue Organic Light-Emitting Diodes Based on Fluorene Derivatives with High Thermal Stability, Adv. Funct. Mater. 15 (2005) p. 1716. https://doi.org/10.1002/adfm.200500067.

[14] C. Yin, D. Zhang, L. Duan, A perspective on blue TADF materials based on carbazole-benzonitrile derivatives for efficient and stable

OLEDs, Appl. Phys. Lett. 116 (2020) p. 120503. https://doi.org/10.1063/1.5143501.

[15] R. Malatong, C. Kaiyasuan, P. Nalaoh, S. Jungsuttiwong, T. Sudyoadsuk, V. Promarak, Rational design of anthracene-based deep-blue emissive materials for highly efficient deep-blue organic light-emitting diodes with CIEy ≤ 0.05, Deyes Pigm. 184 (2021) p. 108874. https://doi.org/10.1016/j.dyepig.2020.108874.

[16] X. Zhu, Y. Li, Z. Wu, C. Lin, D. Ma, Z. Zhao, B.Z. Tang, Anthracene-based bipolar deep-blue emitters for efficient white OLEDs with ultra-high stabilities of emission color and efficiency, J. Mat. Chem. C. 9 (2021) p. 5198.https://doi.org/10.1039/D1TC00432H.

[17] Y.S. Mary, H.T. Varghese, C.Y. Panicker, T. Thiemann, A.A. Al-Saadi, S.A. Popoola, C. Van Alsenoy, Y. Al Jasem, Molecular conformational analysis, vibrational spectra, NBO, NLO, HOMO-LUMO and molecular docking studies of ethyl 3-(E)-(anthracen-9-yl)prop-2-enoate based on density functional theory calculations, Spectrochim. Act. A. 150 (2015) p. 533. https://doi.org/10.1016/j.saa.2015.05.092.

[18] A. Ekbote, P. Patil, S.R. Maidur, T.S. Chia, C.K. Quah, Structural, third-order optical nonlinearities and figures of merit of (E)-1-(3-substituted phenyl)-3-(4-fluorophenyl) prop-2-en-1-one under CW regime: New chalcone derivatives for optical limiting applications, Deyes Pigm. 139 (2017) p. 720. https://doi.org/10.1016/j.dyepig.2017.01.002

[19] P.S. Patil, S.R. Maidur, J.R. Jahagirdar, T.S. Chia, C.K. Quah, M. Shkir, Crystal structure, spectroscopic analyses, linear and third-order nonlinear optical properties of anthracene-based chalcone derivative for visible laser protection, Applied Physics B. 125 (2019) p. 1. https://doi.org/10.1007/s00340-019-7275-z

[20] N.N. Ayare, V.K. Shukla, N. Sekar, Charge transfer and nonlinear optical properties of anthraquinone D-π-A dyes in relation with the DFT based molecular descriptors and perturbational potential, Comput. Thoer. Chem. 1174 (2020) p. 112712. https://doi.org/10.1016/j.comptc.2020.112712

[21] R. Zaier, F. Mahdhaoui, S. Ayachi, T. Boubaker, Prediction of structural, vibrational and nonlinear optical properties of small organic conjugated molecules derived from pyridine, J. Mol. Struct. 1182 (2019) p. 131. https://doi.org/10.1016/j.molstruc.2019.01.043

[22] M. Rajeshirke, N. Sekar, NLO properties of ester containing fluorescent carbazole based styryl dyes – Consolidated spectroscopic and DFT approach Opt. Mater.76 (2018) p. 191. DOI:10.1016/j.optmat.2017.12.035.

[23] J. Zhang, Y. Zhao, H. Xu, D. Zhang, Y. Miao, R. Shinar, J. Shinar, H. Wang, B. Xu, Y. Wu, Novel blue fluorescent emitters structured by linking triphenylamine and anthracene derivatives for organic light-emitting devices with EQE exceeding 5%, J. Mat. Chem. C. 7 (2019) p. 10810. https://doi.org/10.1039/C9TC02773D.

[24] F. Liu, X. Man, H. Liu, J. Min, S. Zhao, W. Min, L. Gao, H. Jin, P. Lu, Highly efficient nondoped blue organic light-emitting diodes with high brightness and negligible efficiency roll-off based on anthracene-triazine derivatives, J. Mat. Chem. C. 7 (2019) p. 14881. https://doi.org/10.1039/C9TC05040J.

[25] S.P. Mishra, A.K. Palai, R. Srivastava, M.N. Kamalasanan, M. Patri, Dithieno[3,2-b:2′,3′-d]pyrrole–alkylthiophene–benzo[c][1,2,5]thiadiazole-based highly stable and low

band gap polymers for polymer light-emitting diodes, J. Poly. Sci. Pol. Chem. 47 (2009) p. 6514. https://doi.org/10.1002/pola.23694.

[26] S.C. Rasmussen, S.J. Evenson, Dithieno[3,2-b,2′,3′-d]pyrrole-based materials: Synthesis and application to organic electronics, Prog. polym. Sci. 38 (2013) p. 1773. https://doi.org/10.1016/j.progpolymsci.2013.04.004.

[27] L. Diao, J. Zhang, R. Wang, G. Liu, S.Pu, Synthesis and properties of asymmetric 9, 10-dithienylanthracene derivatives with AIEE properties and their applications in cell imaging, J. Photochem. Photobio. A. Chem.. 400 (2020) p. 112663. https://doi.org/10.1016/j.jphotochem.2020.112663.

[28] R. Wang, Y. Liang, G. Liu, S. Pu, Aggregation-induced emission compounds based on 9,10-diheteroarylanthracene and their applications in cell imaging, RSC Adv. 10 (2020) p. 2170. DOI: 10.1039/C9RA09290K.

[29] J.K. Fang, D.L. An, K. Wakamatsu, T. Ishikawa, T. Iwanaga, S. Toyota, S. I. Akita, D. Matsuo, A. Orita, J. Otera, Synthesis and spectroscopic study of phenylene–(poly)ethynylenes substituted by amino or amino/cyano groups at terminal(s): electronic effect of cyano group on charge-transfer excitation of acetylenic π-systems, Tetrahedron 66 (2010) p. 5479. https://doi.org/10.1016/j.tet.2010.05.016.

[30] J. George, A. K. Thomas, D. Sajan, S. Sathiyamoorthi, P. Srinivasan, N. Joy, R. Philip, Experimental and DFT/TD-DFT approach on photo-physical and NLO properties of 2, 6-bis (4-Chlorobenzylidene) cyclohexanone, Opt. Mater. 100 (2020) p. 109620. https://doi.org/10.1016/j.optmat.2019.109620

[31] G.W.T.] M.J. Frisch, H.B. Schlegel, G.E. Scuseria, M.A. Robb,, G.S. J.R. Cheeseman, V. Barone, B. Mennucci, G. A. Petersson,, M.C. H. Nakatsuji, X. Li, H.P. Hratchian, A.F. Izmaylov, J. Bloino,, J.L.S. G. Zheng, M. Hada, M. Ehara, K. Toyota, R. Fukuda,, M.I. J. Hasegawa, T. Nakajima, Y. Honda, O. Kitao, H. Nakai, T. Vreven,, J.E.P. J.A. Montgomery Jr., F. Ogliaro, M. Bearpark, J.J. Heyd, E. Brothers,, V.N.S. K.N. Kudin, R. Kobayashi, J. Normand, K. Raghavachari,, J.C.B. A. Rendell, S.S. Iyengar, J. Tomasi, M. Cossi, N. Rega, J. M. Millam,, J.E.K. M. Klene, J.B. Cross, V. Bakken, C. Adamo, J. Jaramillo, R. Gomperts,, O.Y. R.E. Stratmann, A.J. Austin, R. Cammi, C. Pomelli, J.W. Ochterski,, K.M. R.L. Martin, V.G. Zakrzewski, G.A. Voth, P. Salvador,, S. D. J.J. Dannenberg, A.D. Daniels, O. Farkas, J.B. Foresman, J.V. Ortiz,, D.J.F. J. Cioslowski, Gaussian 09 (Revision A.01), Gaussian, Inc., Wallingford, CT.

[32] Z. Lu, P. Dai, C. Wang, M. Liang, X. Zong, Z. Sun, S. Xue, Synthesis of new dithieno[3,2-b:2′,3′-d]pyrrole (DTP) dyes for dye-sensitized solar cells: effect of substituent on photovoltaic properties, Tetrahedron. 72 (2016) p. 3204. https://doi.org/10.1016/j.tet.2016.04.044.

[33] D.C. Santra, M.K. Bera, P.K. Sukul, S. Malik, Charge-Transfer-Induced Fluorescence Quenching of Anthracene Derivatives and Selective Detection of Picric Acid, CHEM-EUR J. 22 (2016) p. 2012. https://doi.org/10.1002/chem.201504126.

[34] R. Zaier, M.P. De La Cruz, F.L. De La Puente, S. Ayachi, Optoelectronic properties of cyclopentadithiophene-based donor–acceptor copolymers as donors in bulk heterojunction organic solar cells: A theoretical study, J. Phys. Chem . Sol. 145 (2020) p. 109532. DOI: 10.1016/j.jpcs.2020.109532.

[35] C. Chitpakdee, S. Namuangruk, P. Khongpracha, S. Jungsuttiwong, R. Tarsang, T. Sudyoadsuk, V. Promarak,

Theoretical studies on electronic structures and photophysical properties of anthracene derivatives as hole-transporting materials for OLEDs, Spectrochim. Act. A. 125 (2014) p. 36. https://doi.org/10.1016/j.saa.2013.12.111.

[36] L. Zhang, W. Shen, R. He, X. Liu, X. Tang, Y. Yang, M. Li, Fine structural tuning of diketopyrrolopyrrole-cored donor materials for small molecule-fullerene organic solar cells: A theoretical study, Org. Elect. 32 (2016) p. 134. https://doi.org/10.1016/j.orgel.2016.01.023.

[37] L. Bhattacharya, S.R. Sahoo, S. Sharma, S. Sahu, Inter. Effect of electron-withdrawing groups on photovoltaic performance of thiophene-vinyl-thiophene derivative and benzochalcogenadiazole based copolymers: A computational study, J. Quant. Chem. 119 (2019) p. e25982. https://doi.org/10.1002/qua.25982.

[38] D. Zhang, X. Song, H. Li, M. Cai, Z. Bin, T. Huang, L. Duan, High-Performance Fluorescent Organic Light-Emitting Diodes Utilizing an Asymmetric Anthracene Derivative as an Electron-Transporting Material, Adv. Mat. 30 (2018) p. 1707590. https://doi.org/10.1002/adma.201707590.

[39] C. Cao, G.X. Yang, J.H. Tan, D. Shen, W.C. Chen, J.X. Chen, J.L. Liang, Z.L. Zhu, S.H. Liu, Q.X. Tong, C.S. Lee, Deep-blue high-efficiency triplet-triplet annihilation organic light-emitting diodes using donor- and acceptor-modified anthracene fluorescent emitters Materials Today Energy. 21 (2021) p. 100727. https://doi.org/10.1016/j.mtener.2021.100727

[40] M.M. Duvenhage, M. Ntwaeaborwa, H.G. Visser, P.J. Swarts, J.C. Swarts, H.C. Swart, Determination of the optical band gap of Alq3 and its derivatives for the use in two-layer OLEDs, Opt. Mater. 42 (2015) p. 193.

https://doi.org/10.1016/j.optmat.2015.01.008.

[41] R. Jin, X. Zhang, W. Xiao, Theoretical Studies of Photophysical Properties of D−π−A−π−D-Type Diketopyrrolopyrrole-Based Molecules for Organic Light-Emitting Diodes and Organic Solar Cells, Molecules. 25 (2020) p. 667. https://doi.org/10.3390/molecules25030667.

[42] S.C. Rasmussen, S.J. Evenson, C.B. McCausland, Fluorescent thiophene-based materials and their outlook for emissive applications, Chem. Comm. 51 (2015) p. 4528. https://doi.org/10.1039/C4CC09206F.

[43] R. Oshi, S. Abdalla, M. Springborg, Study of the influence of functionalization on the reorganization energy of naphthalene using DFT, Comput. Thoer. Chem. 1099 (2017) p. 209. https://doi.org/10.1016/j.comptc.2016.12.002.

[44] R. Zaier, S. Hajaji, M. Kozaki, S. Ayachi, DFT and TD-DFT studies on the electronic and optical properties of linear π-conjugated cyclopentadithiophene (CPDT) dimer for efficient blue OLED, Opt. Mater. 91 (2019) p. 108. https://doi.org/10.1016/j.optmat.2019.03.013.

[45] R. Zaier, S. Ayachi, Toward designing new cyclopentadithiophene-naphthalene derivatives based small molecules for organic electronic applications: A theoretical investigation, Mater Today Commun. (2021) p. 102370. https://doi.org/10.1016/j.mtcomm.2021.102370.

[46] K. Singh, I. Bala, R. Kataria, Crystal structure, Hirshfeld surface and DFT based NBO, NLO, ECT and MEP of benzothiazole based hydrazone, Chem. Phys. 538 (2020) p. 110873. DOI: 10.1016/j.chemphys.2020.110873.

[47] S. Zongo, K. Sanusi, J. Britton, P. Mthunzi, T. Nyokong, M. Maaza, B.

Sahraoui, Nonlinear optical properties of natural laccaic acid dye studied using Z-scan technique, Opt. Mater. 46 (2015) p. 270. https://doi.org/10.1016/j.optmat.2015.04.031.

[48] I. Kucuk, Y. Kaya, A.A. Kaya, Structural, spectroscopic (FT-IR, NMR, UV–visible), nonlinear optical (NLO), cytotoxic and molecular docking studies of 4-nitro-isonitrosoacetophenone (ninapH) by DFT method, J. Mol. Struct. 1139 (2017) p. 308. https://doi.org/10.1016/j.molstruc.2017.03.032.

[49] A. Hussain, M.U. Khan, M. Ibrahim, M. Khalid, A. Ali, S. Hussain, M. Saleem, N. Ahmad, S. Muhammad, A. Al-Sehemi, Structural parameters, electronic, linear and nonlinear optical exploration of thiopyrimidine derivatives: A comparison between DFT/TDDFT and experimental study, J. Mol. Struct. 1201 (2020) p. 127183. https://doi.org/10.1016/j.molstruc.2019.127183

[50] S. Selvakumar, M.S. Boobalan, S.A. Babu, S. Ramalingam, A.L. Rajesh, Crystal growth and DFT insight on sodium *para*-nitrophenolate *para*-nitrophenol dihydrate single crystal for NLO applications, J. Mol. Struct. 1125 (2016) p. 1. https://doi.org/10.1016/j.molstruc.2016.05.104.

[51] S. Muthu, E.I. Paulraj, Molecular structure and spectroscopic characterization of ethyl 4-aminobenzoate with experimental techniques and DFT quantum chemical calculations, Spectrochim. Act. A. 112 (2013) p. 169. https://doi.org/10.1016/j.saa.2013.04.024.

[52] N. Islam, S.S. Chimni, DFT investigation on nonlinear optical (NLO) properties of novel borazine derivatives, Comput. Thoer. Chem. 1086 (2016) p. 58. https://doi.org/10.1016/j.comptc.2016.04.016.

[53] S. Wild, N. Tice, DFT study of structural and electronic properties of 1,4-diarylcyclopenta[d] pyridazines and oxazines for non-linear optical applications, J. Mol. Model. 27 (2021) p. 1. DOI: 10.1007/s00894-021-04676-6.

[54] C.W. Ghanavatkar, V.R. Mishra, N. Sekar, E. Mathew, S.S. Thomas, I.H. Joe, Benzothiazole pyrazole containing emissive azo dyes decorated with ESIPT core: Linear and non linear optical properties, Z scan, optical limiting, laser damage threshold with comparative DFT studies, J. Mol. Str. 1203 (2020) p. 127401. https://doi.org/10.1016/j.molstruc.2019.127401.

[55] R. Jayarajan, R. Satheeshkumar, T. Kottha, S. Subbaramanian, K. Sayin, G. Vasuki, Water mediated synthesis of 6-amino-5-cyano-2-oxo-N-(pyridin-2-yl)-4-(p-tolyl)-2H-[1,2′-bipyridine]-3-carboxamide and 6-amino-5-cyano-4-(4-fluorophenyl)-2-oxo-N-(pyridin-2-yl)-2H-[1,2′-bipyridine]-3-carboxamide – An experimental and computational studies with non-linear optical (NLO) and molecular docking analyses, Spectrochim. Act. A. 229 (2020) p. 117861. https://doi.org/10.1016/j.saa.2019.117861.